On-line Table 1: Sequence technical parameter summary

Parameter	3D-IR GRE MPRAGE	3D-TSE SPACE	3D-GRE VIBE
TR (ms)	2060	600	9.00
TE (ms)	3.66	11.0	3.69
TI (ms)	1040	NA	NA
Fat-suppression technique	Water excitation	Spectral attenuated inversion recovery	Quick-fat saturation
Flip angle	9°	Variable	12°
FOV (mm)	256	256	230
In-plane matrix	256 (read) × 256 (phase)	256 (read) × 256 (phase)	230 (read) × 180 (phase)
Slab thickness (mm)	160	160	160
Slice thickness (mm)	1	1	1
Parallel imaging factor	3×	4×	3×
Acquisition plane	Sagittal	Sagittal	Sagittal
Scan time (min:s)	3:46	3:10	1:57

Note:—NA indicates not applicable; IR, inversion recovery; GRE, gradient recalled-echo.

On-line Table 2: Patients' main demographics and CEL characteristics

Demographics, Characteristics	
No. (with gliomas/metastases)	37 (29/8)
Age (mean) (range) (yr)	57.9 (21–88)
Male/female sex	25/12
Gliomas (No.) (% of all CELs)	38 (70.4%)
Relapsing lesions	16
Histology	
Glioma grade I	2
Glioma grade III	2
Glioma grade IV	31
ODG grade II	2
ODG grade III	1
Metastases (No.) (% of all CELs)	16 (29.6%)
Relapsing lesions	0
Histology	
Lung	7
Breast	3
Melanoma	1
Colorectal	2
Kidney	3

Note:—ODG indicates oligodendroglioma.

On-line Table 3: 1D and 2D measurements

	1D (Median) (IQR) (mm)	*P* (Compared with MPRAGE)[a]	*P* (Adjusted for Sequence Order)[b]	2D (Median) (IQR) (mm^2)	*P* (Compared with MPRAGE)[a]	*P* (Adjusted for Sequence Order)[b]
3D-IR GRE MPRAGE	35.5 (32.7)			860.2 (1996.5)		
3D-TSE SPACE	35.6 (34.3)	<.001[c]	<.001[c]	957 (1889)	.001[c]	.010[c]
3D-GRE VIBE	33.9 (33.9)	.757	.663	847.7 (1796.5)	.750	.069

Note:—IQR indicates interquartile range; IR, inversion recovery; GRE, gradient recalled-echo.
[a] Wilcoxon signed rank test.
[b] General Linear Model
[c] Statistically significant differences.

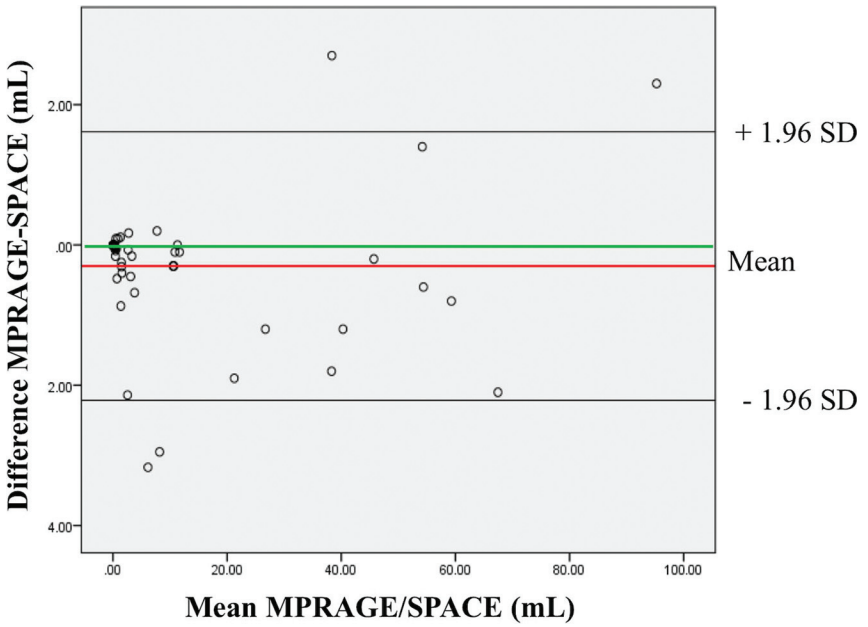

ON-LINE FIG 1. Bland-Altman diagram plotting the differences between MPRAGE and SPACE tumor volume in all lesions. The repeatability coefficient is 2.03 cm^3. Differences above these values are considered significant. The *green line* is the zero line used to assess the discrepancy of the observed mean difference from zero and indicates larger TV measures for SPACE compared with MPRAGE. The *green line* reflects the limits of agreement, and the *red line*, the mean value of the differences.

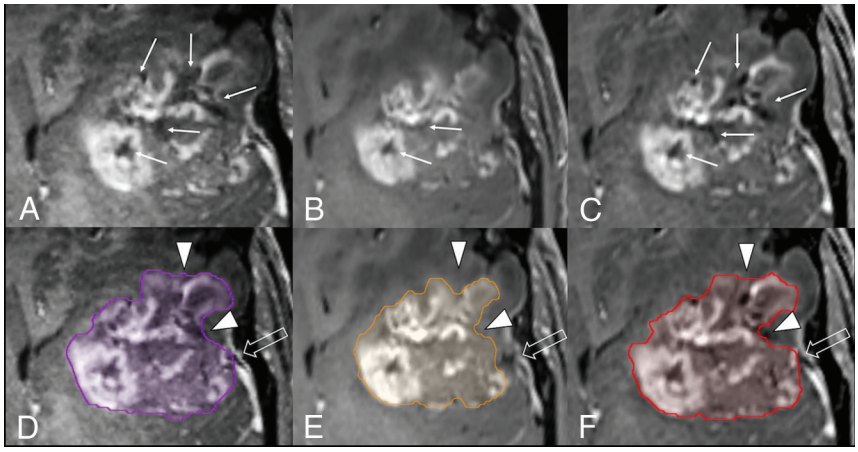

ON-LINE FIG 2. Technique-related differences leading to discrepant enhancement visualization and 3D target object contouring mismatch in a patient with a heterogeneously enhancing glioblastoma *(A*, MPRAGE. *B*, SPACE. *C*, VIBE). Note the small hypointense foci within the lesion, mostly seen on MPRAGE and VIBE (*arrows*), which correspond to susceptibility artifacts related to hemosiderin and/or calcium deposits (see also On-line Fig 3). The corresponding contrast rate/contrast-to-noise ratio values are 95.57/8.31, 110.87/17.94, and 88.54/11.79, while the visual rankings are worst, best, and intermediate, respectively, for MPRAGE, SPACE, and VIBE. The acquisition order was as follows: MPRAGE, VIBE, and SPACE. *D–F*: the corresponding target objects generated by semiautomatic lesion segmentation. A diffuse contouring discrepancy is seen in this case, mainly at the level of the more subtly enhancing tumor borders and of the areas affected by susceptibility artifacts (*arrowheads*, see also On-line Fig 3). Moreover, an overestimation of the tumor border is seen on MPRAGE and VIBE (*D* and *F*) images at the level of the adjacent meningeal vessels (*empty arrows*). On SPACE images (*E*), these vessels appear dark, due to the TSE-related flow void effect, which enabled better separation from the lesion.

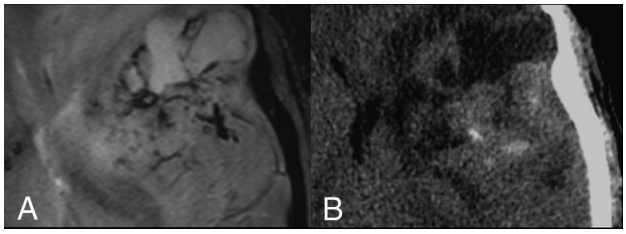

ON-LINE FIG 3. Same case as in On-line Fig 2. The corresponding $T2^*$-weighted image (*A*) and unenhanced CT image (*B*) are presented. These demonstrate intratumoral accumulation of microhemorrhage and calcification deposits with susceptibility effects, resulting in signal loss (*A*).